Supplementary information

Received 21th October 2023,
Accepted 19th December 2023
DOI: 10.1039/d3dt03511e

Lanthanide complexes with a new luminescent iminophosphonamide ligand bearing phenylbenzothiazole substituents

Dmitry K. Sinitsa,[a] Ekaterina K. Pylova,[a,b,c] Olga A. Mironova,[a,*] Denis A. Bashirov,[a]

Alexey A. Ryadun,[a] Taisiya S. Sukhikh,[a] and Sergey N. Konchenko[a,**]

[a]Nikolaev Institute of Inorganic Chemistry SB RAS, Akademika Lavrentieva Ave. 3, 630090 Novosibirsk, Russia.
E-mail: *mironovaoa.nsk@gmail.com **konch@niic.nsc.ru
[b]Department of Natural Sciences, National Research University—Novosibirsk State University, 630090 Novosibirsk, Russia
[c]Institute Charles Gerhardt Montpellier, National School of Chemistry Montpellier, University of Montpellier, CNRS, ENSCM, 34000 Montpellier, France

Table of contents:

Nikolaev Institute of Inorganic Chemistry SB RAS, Akademika Lavrentieva Ave. 3, 630090 Novosibirsk, Russia.
*E-mail: *mironovaoa.nsk@gmail.com **konch@niic.nsc.ru*
† Electronic supplementary information (ESI) available: crystallographic data, NMR spectra, PXRD data for 1, electronic absorption and luminescence spectra of the compounds, scheme of the extraction apparatus, and additional figures of structures. CCDC 2292469-2292473, 2293519 and 2312448. For ESI and crystallographic data in CIF or another electronic format see DOI: See DOI: 10.1039/d3dt03511e

Crystallographic data

Table S1. Crystal data and structure refinement for the compounds

Identification code	**1**	**1**·CH_3CN	**3**·0.5thf·1.5tol	**3***·0.4hexane·1.2tol	**4**·0.5thf·2tol	**5**·3thf·3tol	**6**·4thf·2tol
CCDC Number	2292469	2293519	2292470	2312448	2292473	2292471	2292472
Empirical formula	$C_{38}H_{27}N_4PS_2$	$C_{40}H_{30}N_5PS_2$	$C_{126.5}H_{94}N_{12}O_{0.5}P_3S_6Y$	$C_{124.8}H_{93.0}N_{12}P_3S_6Y$	$C_{130}H_{98}N_{12}O_{0.5}P_3S_6Sm$	$C_{147}H_{126}GdN_{12}O_3P_3S_6$	$C_{144}H_{126}DyN_{12}O_4P_3S_6$
Formula weight	634.72	675.78	2164.31	2134.96	2271.82	2551.11	2536.33
Temperature/K	150(2)	150(2)	150(2)	150(2)	150(2)	150(2)	150(2)
Space group	$P2_1/n$	P21/n	$P2_1/c$	$P2_1/c$	$P2_1/c$	$P2_1/c$	$P2_1/c$
a/Å	9.1902(15)	9.8197(15)	19.092(2)	19.093(2)	19.211(2)	22.7279(6)	22.7471(15)
b/Å	28.224(5)	14.331(2)	14.6554(16)	14.6218(18)	14.6820(14)	14.4740(5)	14.4532(10)
c/Å	11.9753(19)	23.996(3)	38.107(4)	38.215(5)	38.175(4)	38.0128(12)	37.979(3)
β/°	90.930(5)	90.960(5)	94.156(3)	94.667(3)	94.110(3)	93.4490(10)	93.482(3)
Volume/Å^3	3105.8(9)	3376.4(8)	10634(2)	10633(2)	10739.5(18)	12482.2(7)	12463.2(15)
Z	4	4	4	4	4	4	4
ρ_{calc}g/cm^3	1.357	1.329	1.352	1.334	1.405	1.358	1.352
μ/mm^{-1}	0.258	0.243	0.771	0.769	0.768	0.731	0.800
F(000)	1320.0	1408.0	4484.0	4423.0	4676.0	5284.0	5252.0
Radiation	MoKα (λ = 0.71073)	MoKα (λ = 0.71073)	MoKα (λ = 0.71073)	MoKα (λ = 0.71073)	MoKα (λ = 0.71073)	MoKα (λ = 0.71073)	MoKα (λ = 0.71073)
2Θ range for data collection/°	4.462 to 50.048	3.31 to 50.086	3.622 to 49.604	3.622 to 41.63	3.7 to 48.908	3.91 to 54.248	2.882 to 55.848
Index ranges	-10 ≤ h ≤ 10, -33 ≤ k ≤ 33, 0 ≤ l ≤ 14	-11 ≤ h ≤ 11, -16 ≤ k ≤ 17, -28 ≤ l ≤ 28	-22 ≤ h ≤ 21, -17 ≤ k ≤ 17, -39 ≤ l ≤ 44	-18 ≤ h ≤ 19, -14 ≤ k ≤ 14, -38 ≤ l ≤ 38	-22 ≤ h ≤ 22, -17 ≤ k ≤ 17, -44 ≤ l ≤ 44	-29 ≤ h ≤ 29, -18 ≤ k ≤ 18, -48 ≤ l ≤ 48	-29 ≤ h ≤ 29, -19 ≤ k ≤ 19, -42 ≤ l ≤ 50
Reflections collected	5436	39932	94414	47109	104935	223237	109716
Independent reflections	5436 [R_{int} = 0.0613, R_σ = 0.0570]	5951 [R_{int} = 0.1156, R_σ = 0.0763]	18182 [R_{int} = 0.1600, R_σ = 0.1473]	11109 [R_{int} = 0.1596, R_{sigma} = 0.1325]	17657 [R_{int} = 0.1170, R_σ = 0.0812]	27557 [R_{int} = 0.0827, R_σ = 0.0448]	29622 [R_{int} = 0.0577, R_σ = 0.0596]
Restraints/parameters	1/410	1/437	18/1280	11109/195/1333	131/1364	11/1414	10/1398
Goodness-of-fit on F^2	1.127	1.044	1.031	1.017	1.184	1.038	1.019
Final R indexes [I>=2σ (I)]	R_1 = 0.0817, wR_2 = 0.2339	R1 = 0.0549, wR2 = 0.1289	R_1 = 0.0902, wR_2 = 0.1956	R_1 = 0.0718, wR_2 = 0.1527	R_1 = 0.0841, wR_2 = 0.1753	R_1 = 0.0454, wR_2 = 0.1080	R_1 = 0.0517, wR_2 = 0.1305
Final R indexes [all data]	R_1 = 0.0969, wR_2 = 0.2433	R1 = 0.0773, wR2 = 0.1444	R_1 = 0.1637, wR_2 = 0.2303	R_1 = 0.1349, wR_2 = 0.1838	R_1 = 0.1113, wR_2 = 0.1860	R_1 = 0.0578, wR_2 = 0.1157	R_1 = 0.0701, wR_2 = 0.1419
Largest diff. peak/hole / e Å^{-3}	0.37/-0.55	0.31/-0.37	1.33/-1.10	0.74/-0.60	1.92/-1.36	1.06/-0.93	1.80/-0.92

Spectroscopy & PXRD data

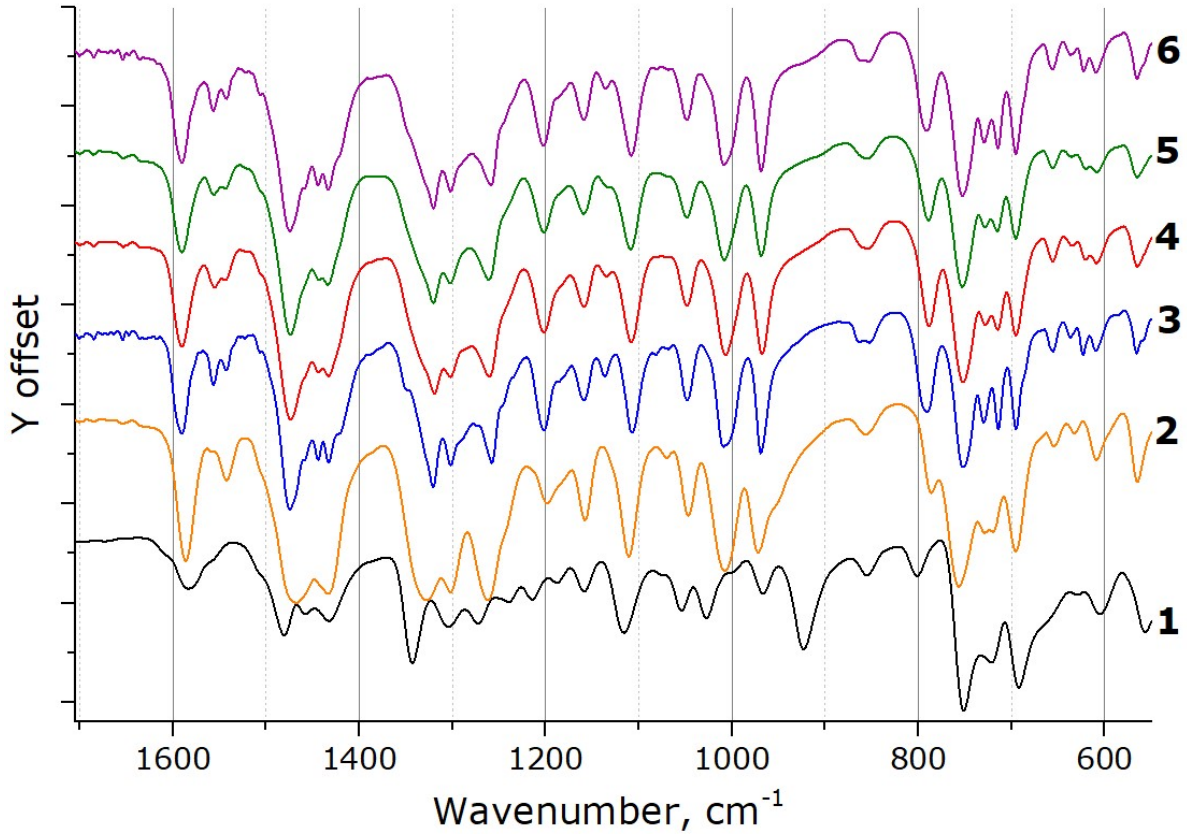

Figure S1. IR spectra of compounds **1**-**6**.

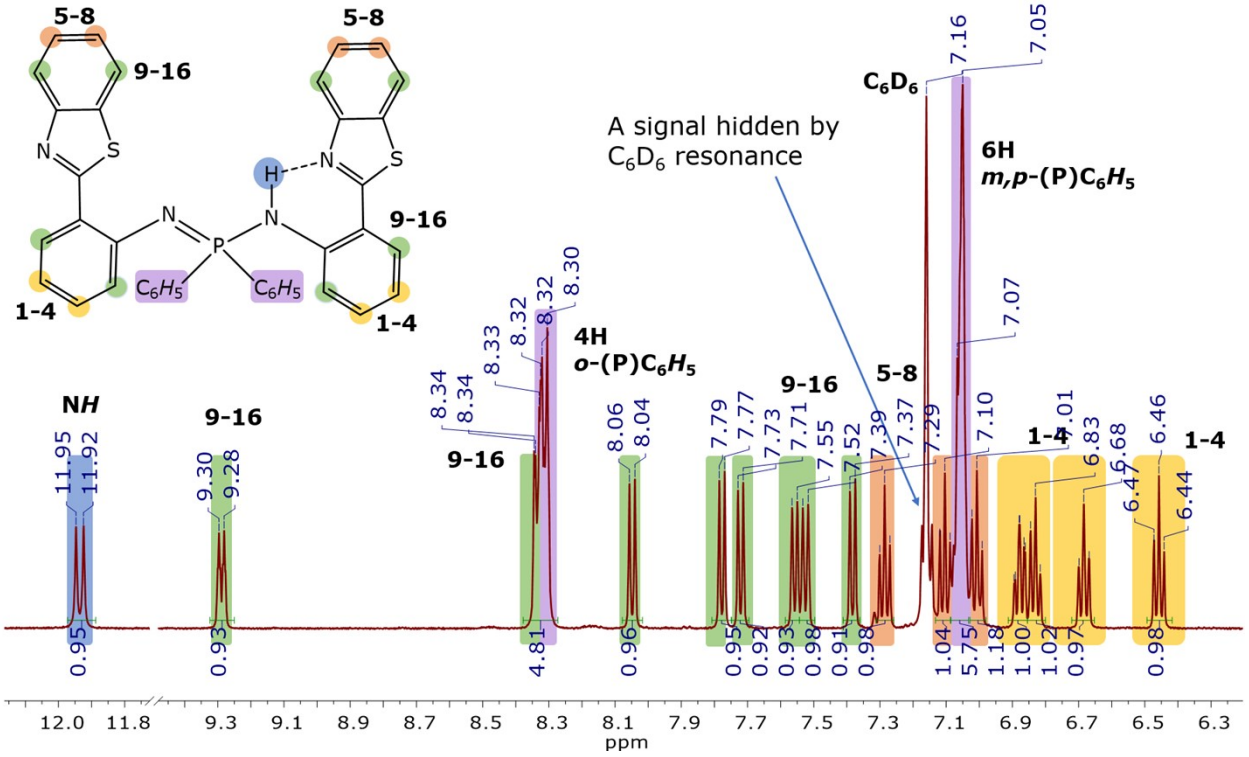

Figure S2. ^{1}H NMR spectrum of **1** in benzene-d_6.

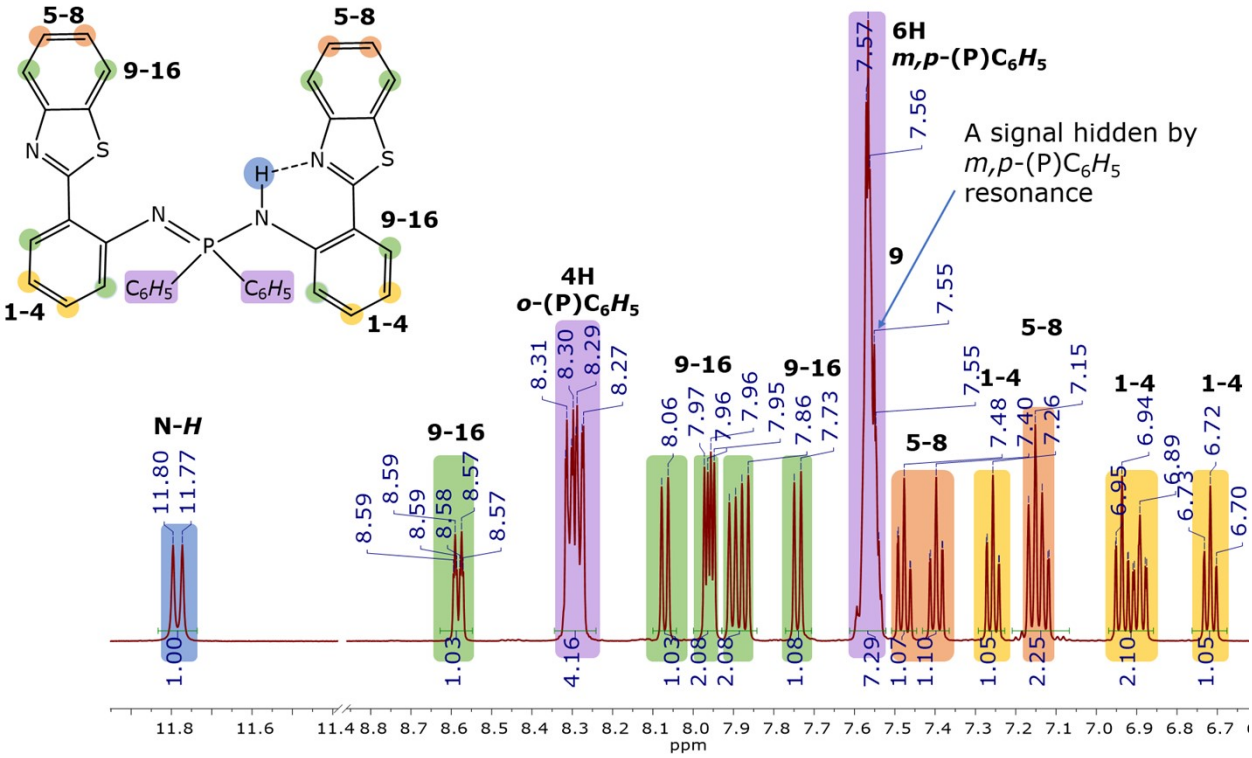

Figure S3. ^{1}H NMR spectrum of **1** in thf-d_8.

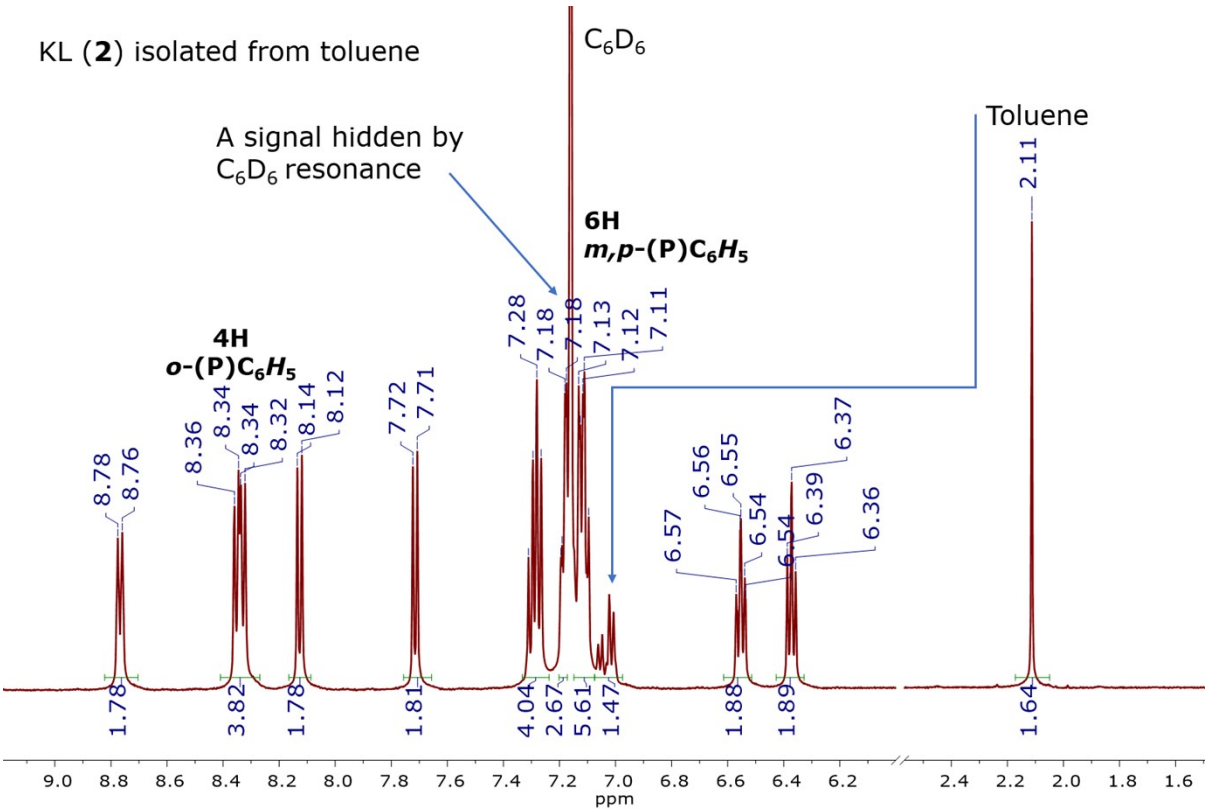

Figure S4. ^{1}H NMR spectrum of **2** in benzene-d_6.

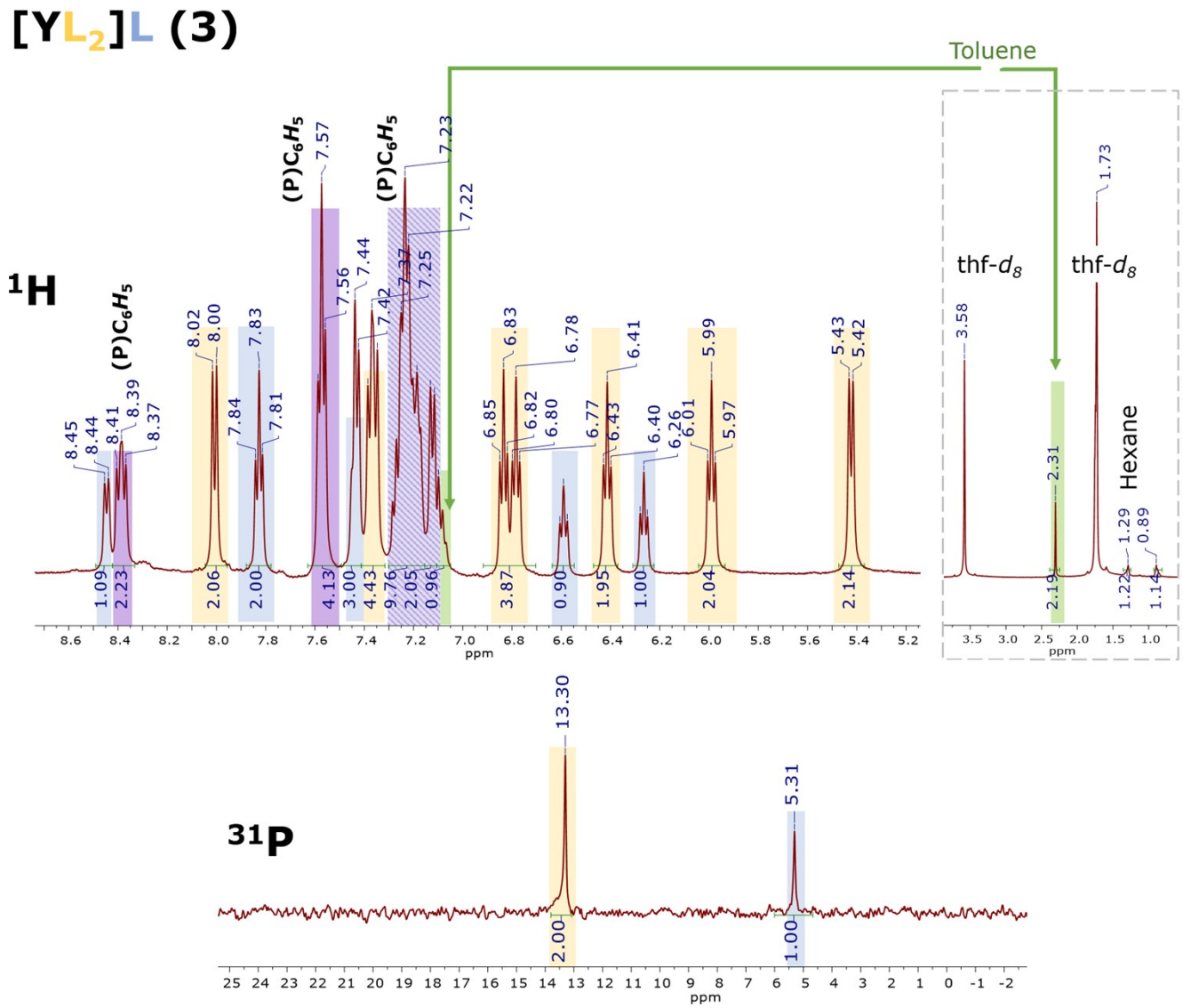

Figure S5. An approximate assignment of signals in the ^{1}H NMR and ^{31}P spectra of **3** in thf-d_8.

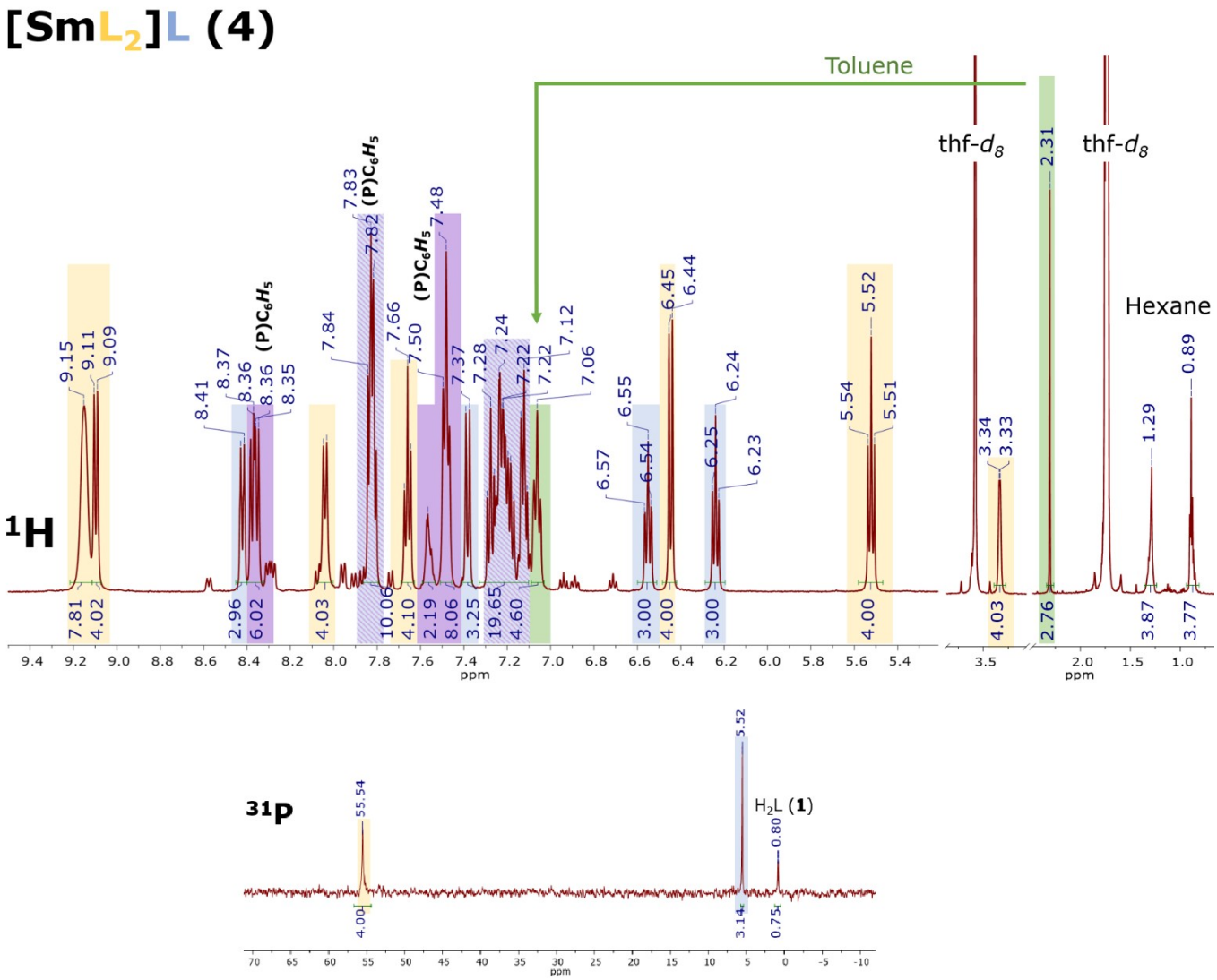

Figure S6. An approximate assignment of signals in the ^{1}H NMR and ^{31}P spectra of **4** in thf-d_8. Another ratio coordinated : outer-sphere ligand may be caused by solvation or ligand redistribution effects.

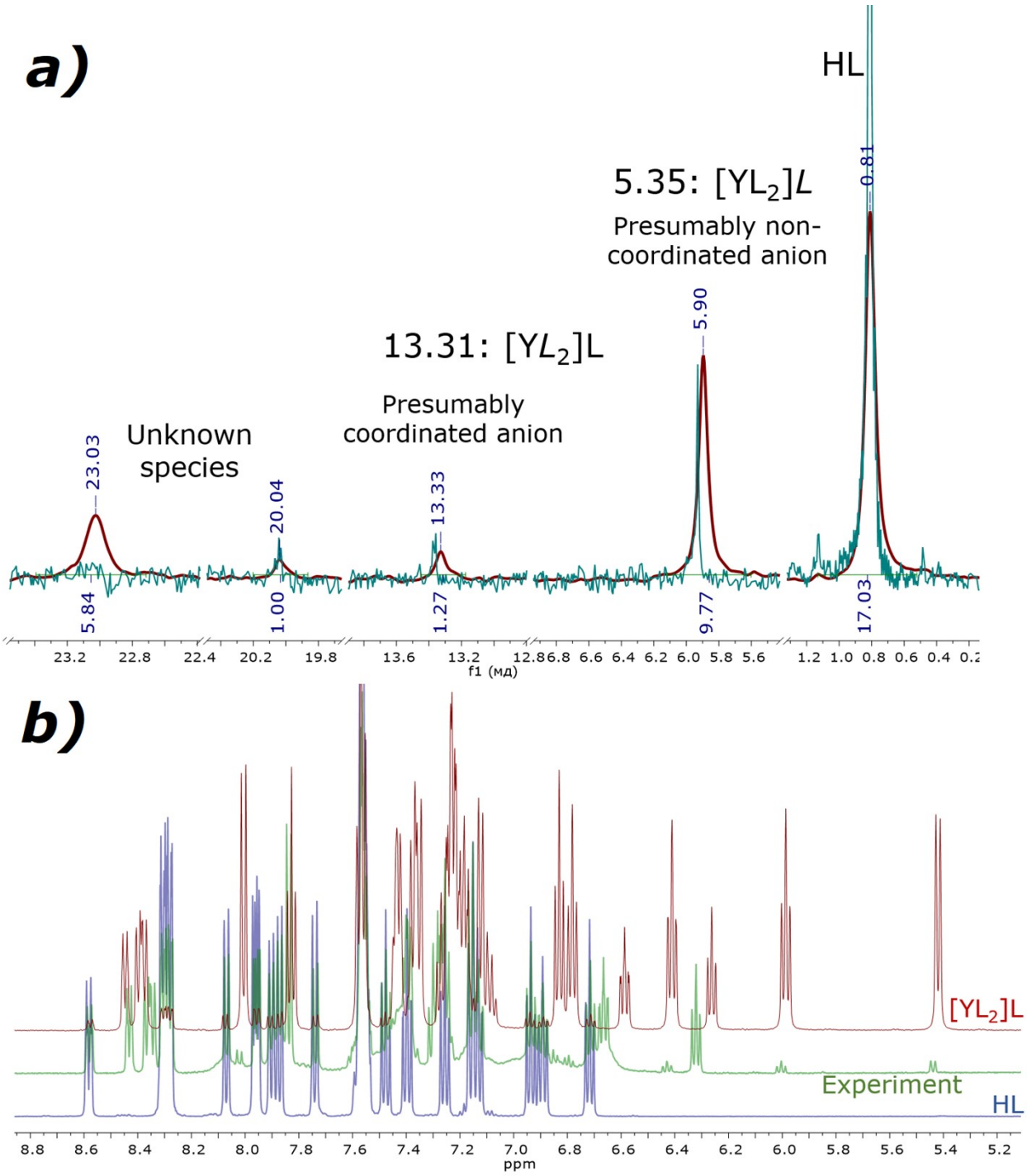

Figure S7. An approximate assignment of signals in the NMR experiment *a*) ^{31}P (green: two days, 55°C; vinous: three days more, 70°C) and *b*) ^{1}H NMR spectrum in thf-d_8.

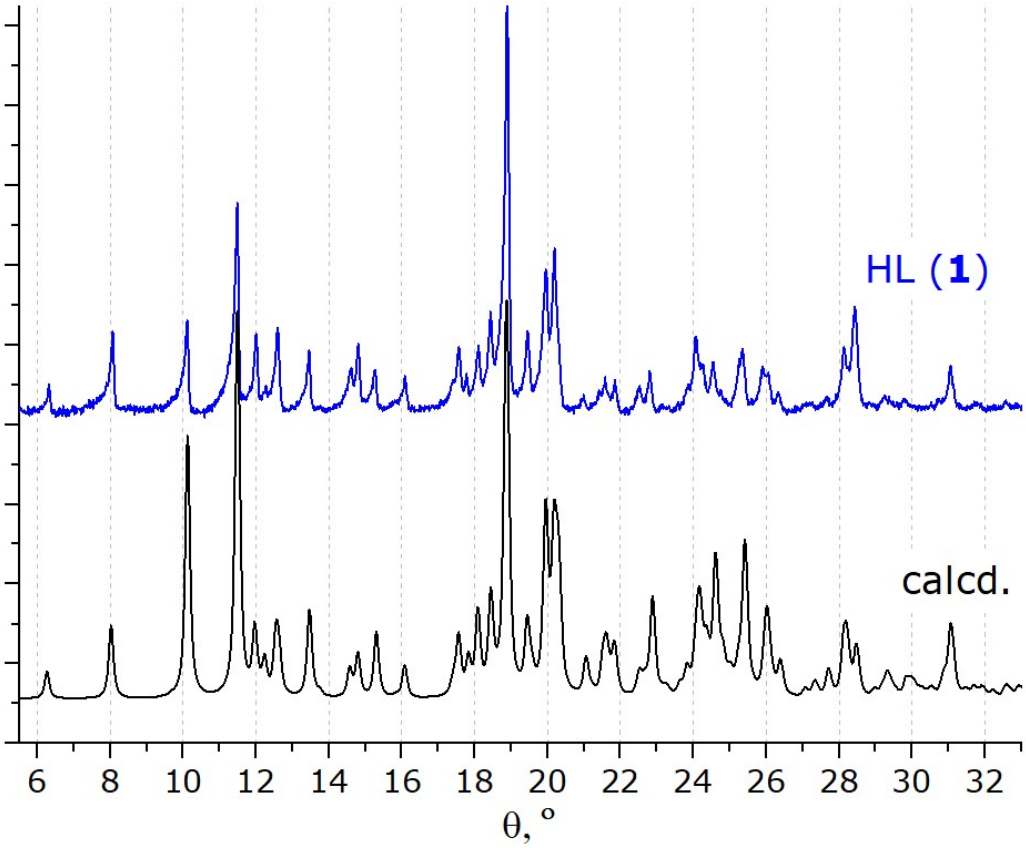

Figure S8. Powder pattern of **1**.

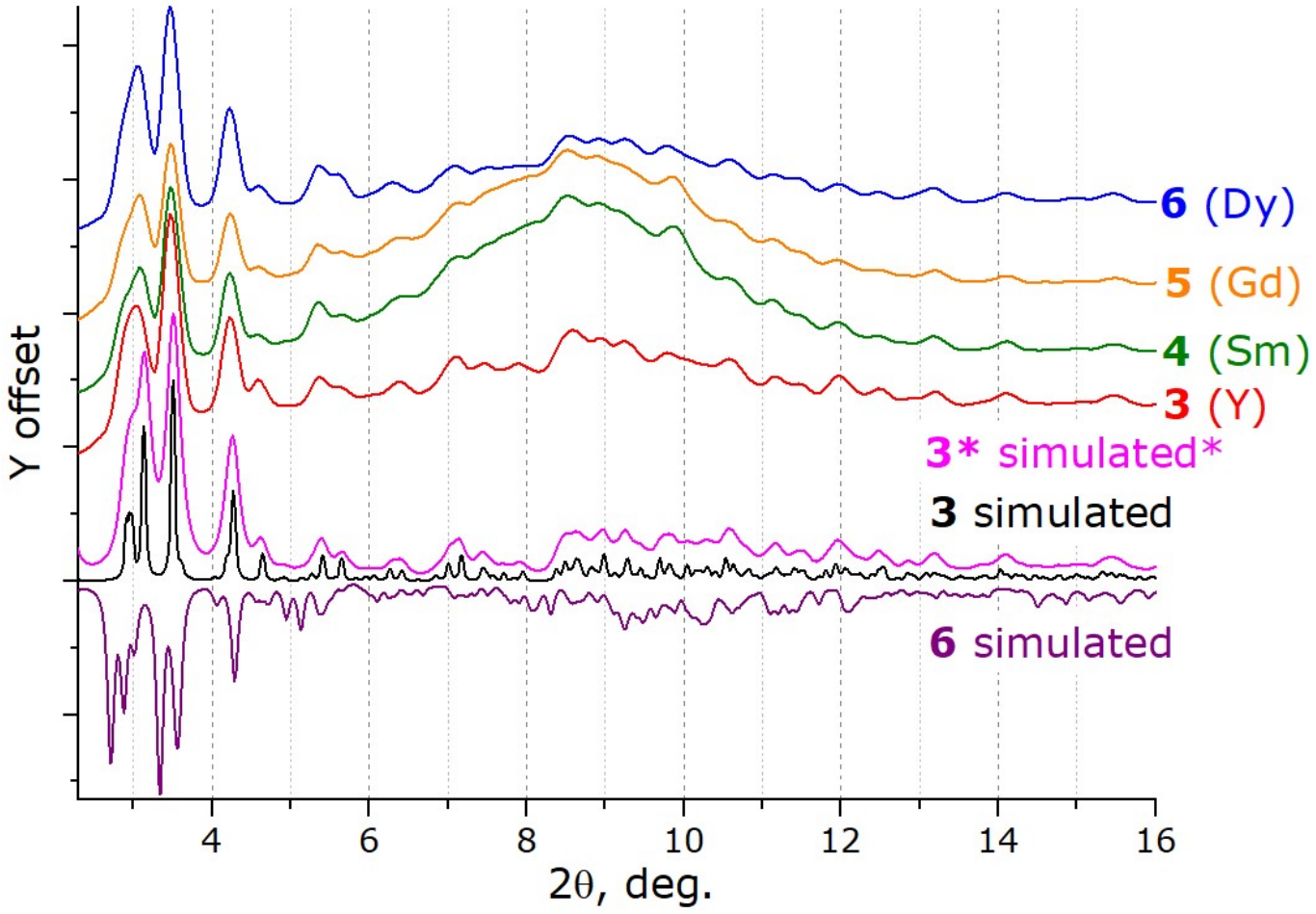

Figure S9. Powder patterns of compounds **3**-**6** (MoKα radiation, λ = 0.70932 Å) measured for crystalline powders placed into perfluorinated oil. The halo at angles of 8–10° is due to the contribution of oil. Peaks below 2.4° are hidden by the beamstop, no prominent peaks are observed above 16° in the simulated and obtained powder patterns. Theoretical powder patterns for **3** and **4**, **5** and **6** are pairwise similar. The theoretical powder pattern for **3*** is given with FWHM = 0.2 for illustrative purposes, for **3** and **6** FWHM = 0.1.

Photophysical measurements

Table S2. Absorption maxima and molar extinction coefficients of **1**, **2**, **5**, and **6** in thf solution.

Compound	λ, nm	ε, 10^{-4} $M^{-1}cm^{-1}$	Compound	λ, nm	ε, 10^{-4} $M^{-1}cm^{-1}$
1	230	7.37	**2**	232	6.24
	258	3.21		260	3.33
	283*(sh)*	2.77		284*(sh)*	3.10
	296	3.04		297	3.11
	309*(sh)*	2.41		369*(br)*	1.51
	361*(br)*	2.85		422*(br)*	2.08
4	230	20.17	**5**	232	15.40
	262	10.78		261	8.25
	299	9.25		299	7.33
	312*(sh)*	8.06		314*(sh)*	5.85
	375*(sh)*	4.68		381*(sh)*	3.57
	403*(br)*	4.92		406*(br)*	4.06
	427*(sh)*	4.02		423*(sh)*	3.82
6	230	16.64			
	261	8.31			
	298	7.41			
	312*(sh)*	6.21			
	368*(br)*	4.13			
	405	3.01			
	424*(br, sh)*	2.64			

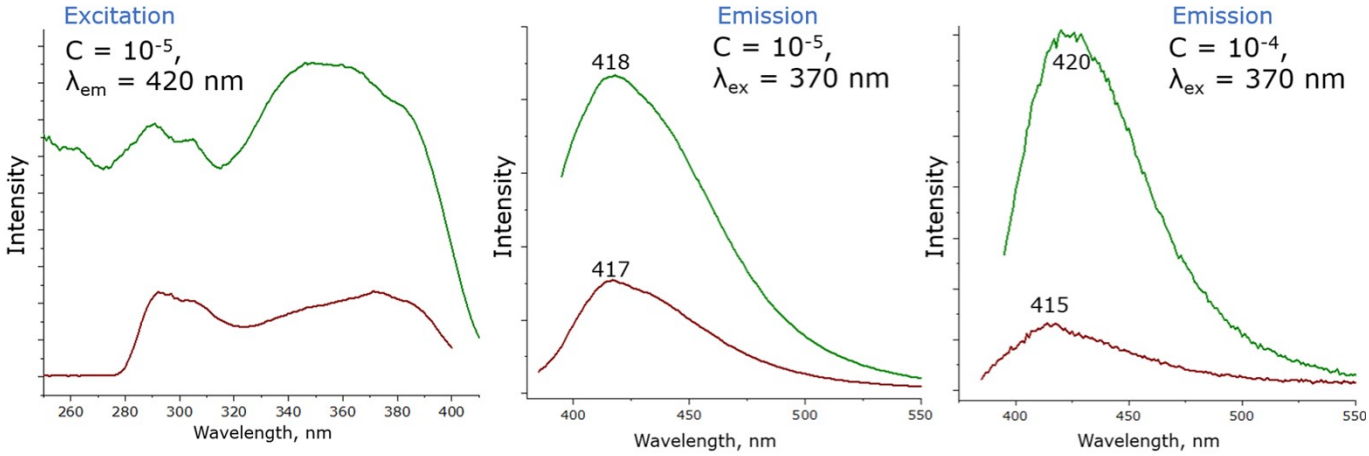

Figure S10. Luminescence and excitation spectra of **1** in thf (green) and toluene (vine red) solutions of different concentrations.

Table S3. Coordinates* of HL luminescence colour at the chromaticity diagram upon the corresponding excitation. *The calculation accuracy may be decreased for the 410-430 nm range of excitation because of the overlay of excitation and emission regions.

λ_{ex}, nm	350	360	370	380	390	400	410	420	430
x	0.34517	0.32682	0.31654	0.30838	0.28227	0.27166	0.27267	0.23561	0.19947
y	0.23201	0.21736	0.2051	0.19173	0.16487	0.1553	0.16615	0.17701	0.21675

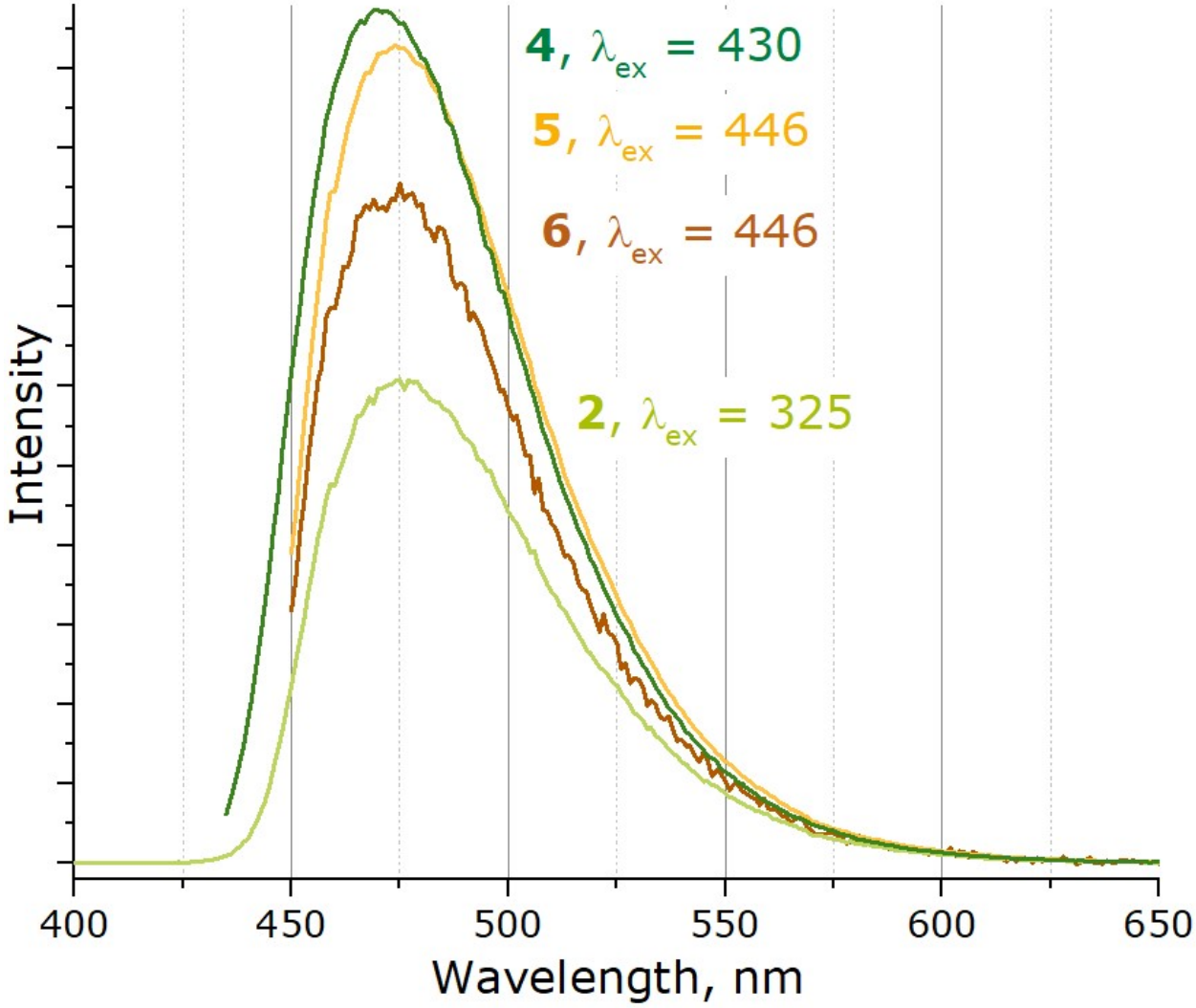

Figure S11. Luminescence spectra of thf solutions of compounds **2**, **4**, **5**, **6**, measured on Cary Eclipse. Slit wides 2.5×2.5, C(**2**, **6**) = $1.2 \cdot 10^{-4}$ M, C(**4**) = $1.3 \cdot 10^{-4}$ M, C(**5**) = $9.9 \cdot 10^{-5}$ M.

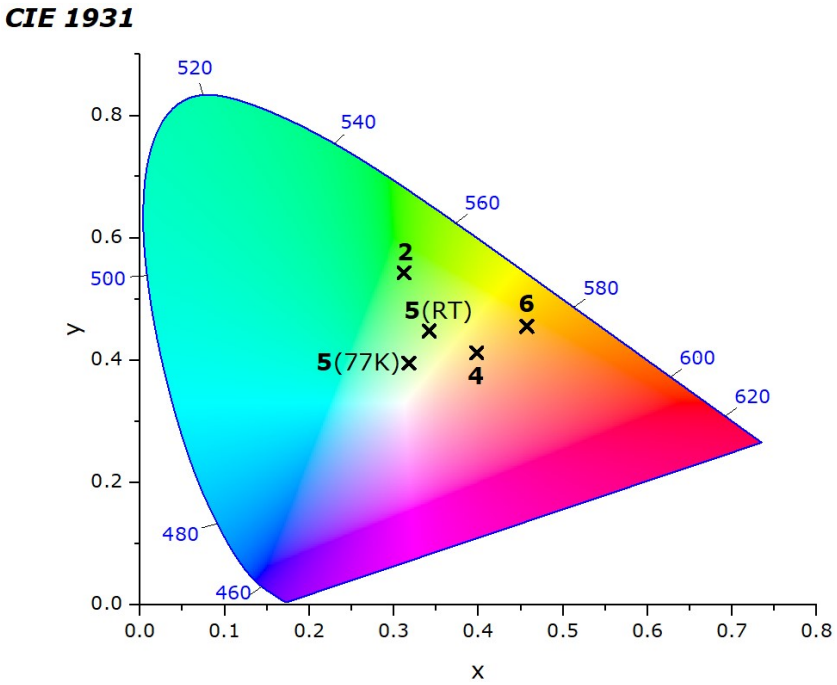

Figure S12. Positions of **2**, **4**-**6** luminescence colour coordinates on CIE 1931 diagram.

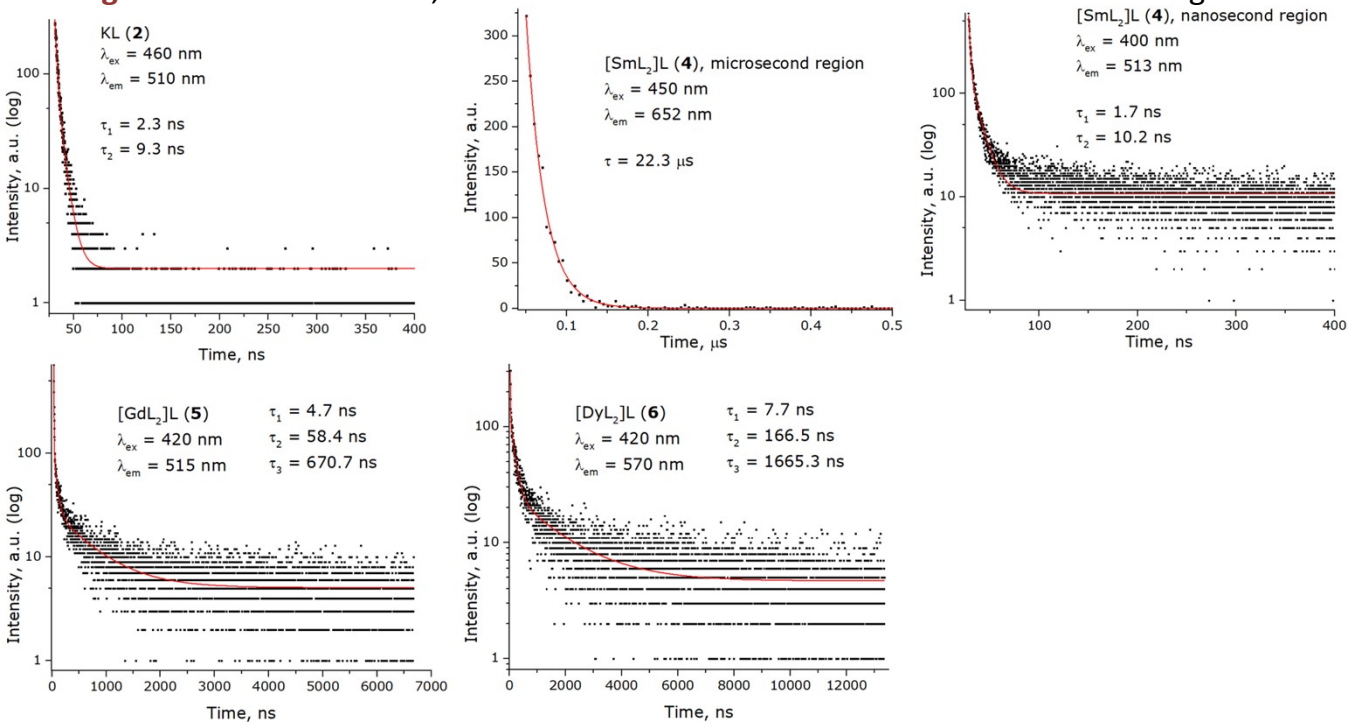

Figure S13. Decay curves of **2**, **4**-**6** luminescence.

Additional information

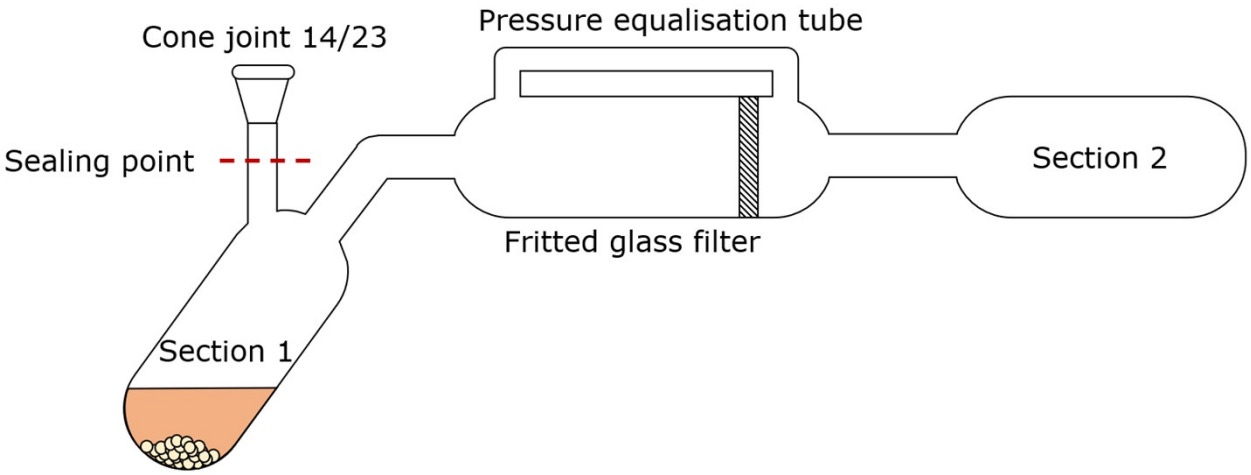

Figure S14. Extraction apparatus.

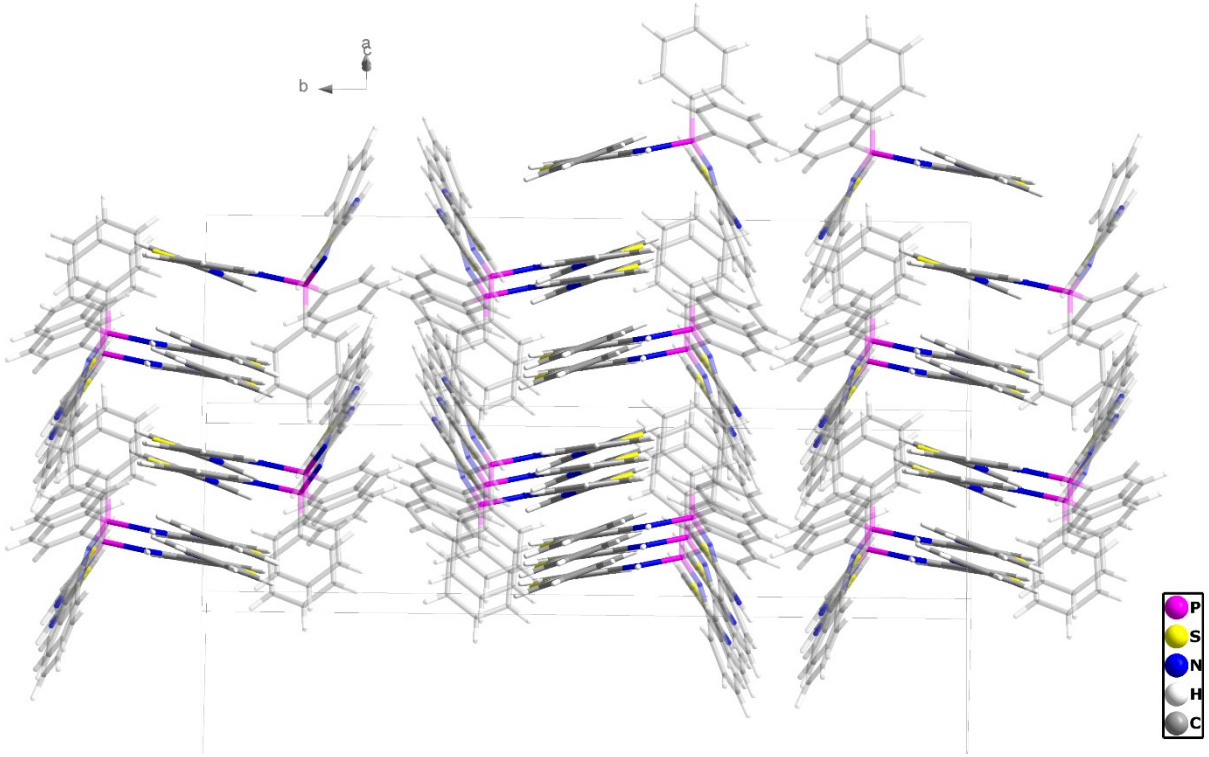

Figure S15. Packing of **1**, conditioned by π-stacking.

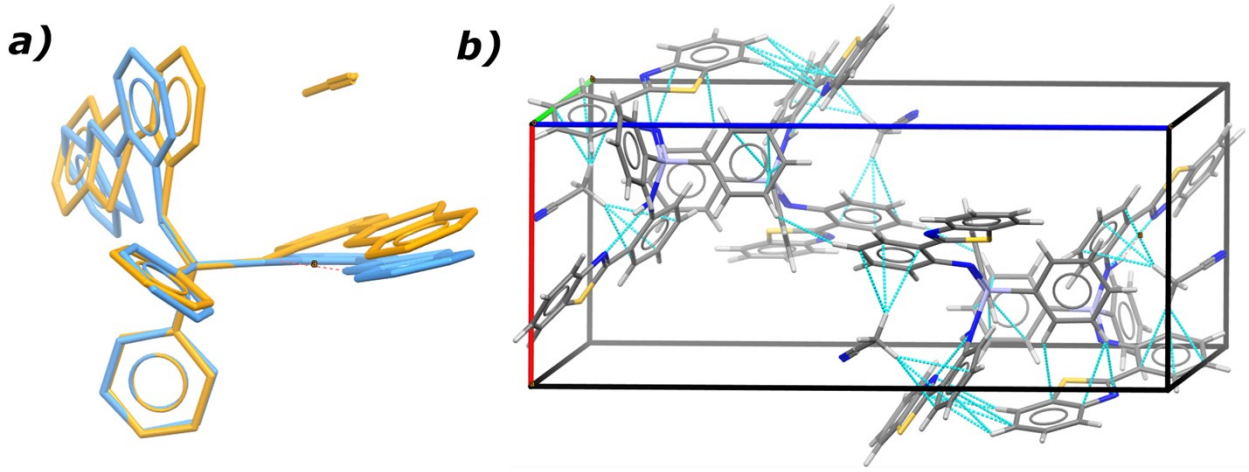

Figure S16. *a*) Overlay of molecules of HL in the structures of the solvent-free **1** and **1**·CH_3CN; *b*) Packing of **1**·CH_3CN.

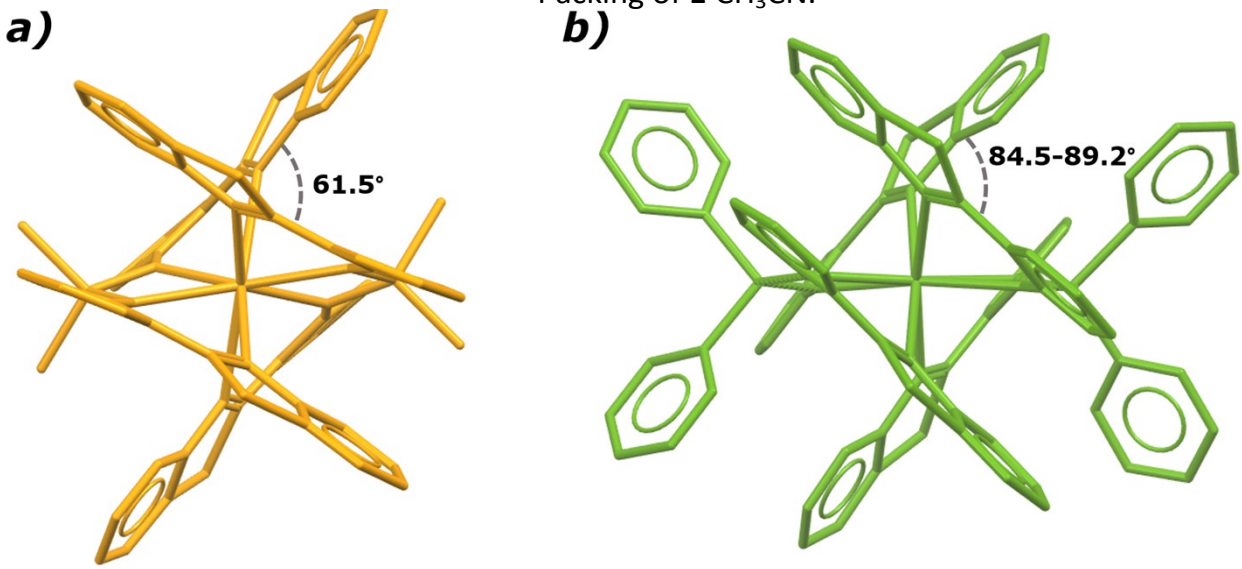

$[Y(SiMe_2(NPbt)_2)_2]^+$ $[Y(PPh_2(NPbt)_2)_2]^-$

Figure S17. Comparison of $[YL_2]$ units.

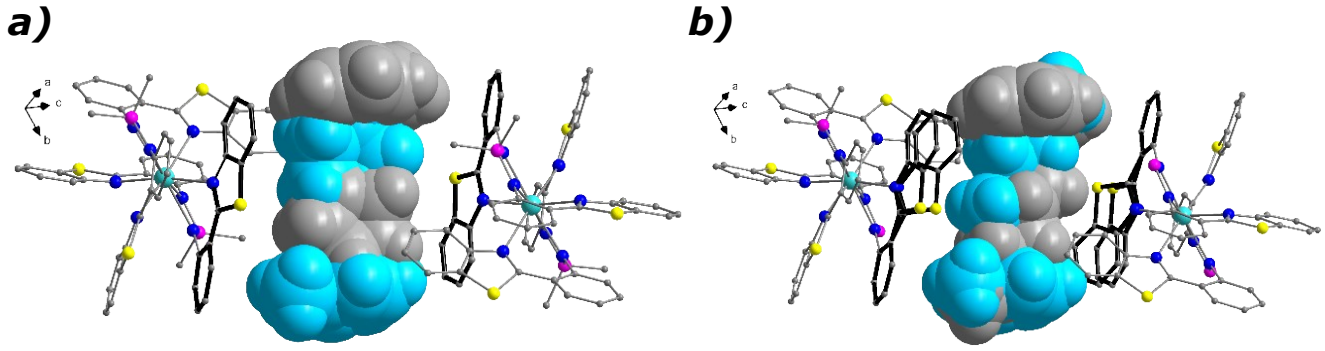

Figure S18. Comparison of a fragment of the structures of *a)* **3**·0.5thf·1.5tol and *b)* **3***·0.4hexane·1.2tol revealing a slight variation in the positions of disordered solvent molecules. The different positions are shown as grey and blue spheres; the closest to them Pbt moieties are bolded. H atoms are omitted except for those in the solvent molecules.

According to single-crystal XRD analysis, the compounds reveal the presence of a cavity that can accommodate up to one toluene and one thf or hexane molecule disordered over proximate positions. This brings a slight variation in the crystal composition. By the example of the Y compound, we traced that the dried sample (**Figure S18b**) comprises approximately the same number of solvent molecules as in the as-synthesized crystal (**Figure S18a**). Notably, the closest to the cavity Pbt moieties can also show some disorder caused by a variation in nature and/or the number of solvent molecules.

According to ^{1}H NMR spectroscopy, the sample of **3** contains hexane but not thf molecules. Thus, we speculate that the thf is replaced with hexane upon isolation of the products.